

# Chemical evolution of Damped Ly $\alpha$ galaxies: The [S/Zn] abundance ratio at redshift $\geq 2$ <sup>1</sup>

Miriam Centuri3n, Piercarlo Bonifacio, Paolo Molaro, and Giovanni Vladilo

Osservatorio Astronomico di Trieste, Via G.B. Tiepolo 11, 34131, Trieste

Received \_\_\_\_\_; accepted \_\_\_\_\_

arXiv:astro-ph/0001109v1 7 Jan 2000

---

<sup>1</sup>Based on observations made with the William Herschel telescope operated on the island of La Palma by Isaac Newton Group in the Spanish Observatorio del Roque de Los Muchachos of the Instituto de Astrofísica de Canarias, and on observations collected with the ESO 3.6m telescope at the European Southern Observatory, Chile.

## ABSTRACT

Relative elemental abundances, and in particular the  $\alpha/\text{Fe}$  ratio, are an important diagnostic tool of the chemical evolution of damped Ly  $\alpha$  systems (DLAs). The S/Zn ratio is not affected by differential dust depletion and is an excellent estimator of the  $\alpha/\text{Fe}$  ratio. We report 6 new determinations of sulphur abundance in DLAs at  $z_{\text{abs}} \geq 2$  with already known zinc abundances. The combination with extant data from the literature provides a measure of the S/Zn abundance ratio for a total of 11 high redshift DLA systems. The observed [S/Zn] ratios do not show the characteristic [ $\alpha/\text{Fe}$ ] enhancement observed in metal-poor stars of the Milky Way at comparable level of metallicity ([Zn/H]  $\approx -1$ ). The behaviour of DLAs data is consistent with a general trend of decreasing [S/Zn] ratio with increasing metallicity [Zn/H]. This would be the first evidence of the expected decrease of the  $\alpha/\text{Fe}$  ratio in the course of chemical evolution of DLA systems. However, in contrast to what observed in our Galaxy, the  $\alpha/\text{iron-peak}$  ratio seems to attain solar values when the metallicity is still low ([Zn/H]  $\leq -1$ ) and to decrease below solar values at higher metallicities. The behaviour of the  $\alpha/\text{Fe}$  ratio challenges the frequently adopted hypothesis that high redshift DLAs are progenitors of spiral galaxies and favours instead an origin in galaxies characterized by low star formation rates, in agreement with the results from imaging studies of low redshift DLAs, where the candidate DLA galaxies show a variety of morphological types including dwarfs and LSBs and only a minority of spirals.

*Subject headings:* cosmology: observations — galaxies: abundances — galaxies: evolution — quasars: absorption lines

## 1. Introduction

Damped Lyman  $\alpha$  systems are QSO absorbers with the highest values of neutral hydrogen column density ( $\log N(\text{HI}) \geq 20.3$  atoms/cm<sup>-3</sup>). The Ly $\alpha$  absorption profiles show extended "radiation damping" wings (hence their name) and are always associated with narrow metal absorptions. Even though it is generally agreed that DLA absorbers at high redshifts originate in proto-galaxies located in the direction of the background QSO, the nature of such intervening galaxies is still subject of debate.

The analysis of the kinematics of the metal lines has suggested that DLAs arise in massive rotating disks which are the progenitors of the present-day spiral galaxies (Wolfe et al. 1995, Prochaska & Wolfe 1997,1999). However, other works indicate that the observed kinematical properties can be equally explained by low-mass proto-galactic objects (Haehnelt, Steinmetz, & Rauch 1998; Ledoux et al. 1998).

The imaging of galaxies in the field of the background QSOs indicates that at  $z_{\text{abs}} \leq 1$  — where this technique can be applied — the population of DLA galaxies is not dominated by a specific morphological type, and, in particular, spirals constitute a small fraction of the sample (Le Brun et al. 1997; Rao & Turnshek 1998).

Abundance studies of DLAs have also the potential to provide independent clues to understand the nature of this class of QSO absorbers. Abundances determinations have already been obtained for about 60 systems, mainly at  $z_{\text{abs}} > 1.7$ , (Lu et al. 1996; Pettini et al. 1997,1999; Prochaska & Wolfe 1999, hereafter PW99). DLA galaxies show low metallicities — typically 10% of solar — comparable with the metallicity level measured in metal-poor stars of the Galactic halo. Although the precision obtained in DLA's abundance determinations is remarkable and often comparable to that attained in the Galactic ISM, the interpretation of the observed abundance ratios has led to contradictory conclusions.

If DLA galaxies are protospirals and have experienced a chemical evolution similar to that of our Galaxy, we expect to observe the elemental abundance pattern typical of halo stars of comparable metallicity. In particular, we expect to observe the enhancement of  $\alpha$  over iron-peak elements ratio  $[\alpha/\text{Fe}]^2 \simeq +0.5$  characteristic of Galactic metal poor stars (Ryan, Norris, & Beers 1996). The only  $[\alpha/\text{Fe}]$  ratio with a large number of determinations in DLAs is  $[\text{Si}/\text{Fe}]$ . The mean value  $\langle [\text{Si}/\text{Fe}] \rangle \simeq +0.4 \pm 0.2$  is consistent with the typical value of the Galactic halo stars and has been interpreted as evidence for an origin of DLAs in proto-spirals (Lu et al. 1996, PW99). However, also in the nearby interstellar medium

---

<sup>2</sup>Using the standard definition  $[\text{X}/\text{Y}] = \log(\text{X}/\text{Y}) - \log(\text{X}/\text{Y})_{\odot}$

one typically finds  $\langle[\text{Si}/\text{Fe}]\rangle \simeq +0.4$  owing to differential elemental depletion onto dust grains (Savage & Sembach 1996). Vladilo (1998) obtained intrinsic solar ratios ( $[\text{Si}/\text{Fe}] \approx 0$ ) in DLAs after correction for the differential elemental depletion. Also Pettini et al. (1999) have recently found solar Si/Zn ratios in 3 DLAs by taking into account dust effects.

By using ratios of undepleted elements such as  $[\text{S}/\text{Zn}]$ , Molaro et al. (1996) and Molaro, Centuri3n, & Vladilo (1998; hereafter MCV98) also obtained solar ratios, in spite of the low metallicity of the DLAs investigated. Since sulphur and zinc are essentially undepleted in the interstellar medium, the  $[\text{S}/\text{Zn}]$  ratio is probably the best diagnostic of the  $[\alpha/\text{Fe}]$  ratio available for DLAs. However, only a few measurements of sulphur abundances are available owing to the difficulty of observing the SII resonant triplet in the Ly  $\alpha$  forest. For this reason we have performed a search for SII in DLAs. Here we present the results of this search in 7 DLAs with known ZnII abundances. We obtain 4 sulphur abundance measurements and 2 limits, which allow us to enlarge significantly the sample of  $[\text{S}/\text{Zn}]$  determinations.

## 2. Observations and data reduction

The QSOs observed in the course of the present investigation are listed in Table 1, together with relevant information concerning the observations. The spectra of QSO 0013-004 and QSO 2231-0015 were obtained with the CASPEC echelle spectrograph at the Cassegrain focus of ESO 3.6m telescope at La Silla, Chile. The spectra of the remaining QSOs were obtained with the two arms ISIS spectrograph at the Cassegrain focus of the William Herschel Telescope (WHT, 4.2m.) at La Palma, Canary Islands.

For the CASPEC observations we used the echelle grating of 31.6 grooves/mm and a Tektronix CCD with 1024x1024 square pixels of 24  $\mu\text{m}$  in size. The CCD was binned at a step of 2 pixels along the dispersion direction and the slit width was set at 2.1 arcsec in order to have the projection onto 2 binned pixels of the detector. The slit width matched the seeing, which was around 2 arcsecs during the observations at La Silla.

For the observations performed with ISIS blue arm we used a 1200 grooves/mm grating coupled with an EEV CCD with 2048 x 4200 square pixels of 13.5  $\mu\text{m}$  in size. The CCD was binned in the spatial and dispersion directions at step of 2 x 2 pixels. The slit width was set at 1 arcsec. This value still allows a correct sampling of the spectrum without any loss in resolution thanks to the small pixel size of the EEV CCD.

The full width at half maximum of the instrumental profile sampled with 2 binned pixels,  $\Delta\lambda_{instr}$ , was measured from the emission lines of the Thorium-Argon lamp (CASPEC) and from the Copper-Argon plus Copper-Neon lamps (ISIS blue arm) recorded contiguously to each target exposure. The resulting resolving power  $R = \lambda/\Delta\lambda_{instr}$  was  $R \simeq 19000$  for CASPEC spectra and  $\simeq 5000$  in the sulphur region of ISIS blue data, corresponding to a velocity resolution of  $\Delta v \simeq 16 \text{ km s}^{-1}$  and  $60 \text{ km s}^{-1}$ , respectively.

The data reduction was performed using the ECHELLE (CASPEC spectra) and LONG (ISIS spectra) routines implemented in the software package MIDAS developed at ESO. The first steps of the reduction procedure — including flat-fielding, cosmic ray removal, sky subtraction, optimal extraction, and wavelength calibration — were performed separately on the different spectra of each QSO. Typical internal errors in the wavelength calibrations are of  $\simeq 4 \text{ m}\text{\AA}$  for CASPEC spectra and  $\simeq 30 \text{ m}\text{\AA}$  for ISIS blue data.

The observed wavelength scale of the spectra was then transformed into vacuum, heliocentric wavelength scale. At this point the different spectra of each QSO were averaged, using as weights the continuum levels of the exposures. Finally, for each spectral range under study the local continuum was determined in the average spectrum by using a spline to smoothly connect the regions free from absorption features. The final spectrum used for the analysis was obtained by normalising the average spectrum to these continua. The signal-to-noise ratios per pixel of the extracted final spectra, estimated from the *rms* scatter of the continuum near the absorptions under study, are typically in the range between 10 and 25.

In addition to the SII triplet at  $1254\text{\AA}$ , our data also cover, in general, the spectral regions of NI multiplets ( $1134, 1200 \text{\AA}$ ), and the transitions of OI( $1302, 1355\text{\AA}$ ), SiIII ( $1190, 1193, 1260, 1304, 1526\text{\AA}$ ) and FeII ( $1121, 1125, 1127, 1133, 1143, 1144 \text{\AA}$ ). In this paper we focus our attention on the new measurements of the SII triplet. When possible, we used other lines to obtain information that could be used to constrain the SII column densities. We do not report OI column densities because the transition at  $\lambda 1302\text{\AA}$  is heavily saturated, while the extremely weak OI  $1356 \text{\AA}$  line is not detected and provides no stringent upper limits. Nitrogen abundance determinations in these DLAs will be discussed in a subsequent paper.

### 3. Column densities

Column densities have been obtained by fitting theoretical Voigt profiles to the observed absorption lines via  $\chi^2$  minimization. This step was performed using the routines FITLYMAN (Fontana & Ballester 1995) included in the MIDAS package. During the fitting procedure the theoretical profiles were convolved

with the instrumental point spread function modeled from the analysis of the emission lines of the arcs. Portions of the profiles contaminated by intervening Ly  $\alpha$  absorbers were excluded from the fit.

The FITLYMAN routines determine the redshift, the column density (atoms  $\text{cm}^{-2}$ ), and the broadening parameter ( $b$ -value)<sup>3</sup> of the absorption components, as well as the fit errors for each one of these quantities. In addition, we estimated errors due to the uncertainty in the continuum placement, as we explain in the rest of this section.

Measurements of SII column densities were derived from the three lines at  $\lambda\lambda 1250.584, 1253.811, 1259.519 \text{ \AA}$  with oscillator strengths  $f_\lambda=0.00545, 0.01088, 0.01624$  respectively. All the atomic data used in this work are from Morton (1991). The SII triplet is generally unsaturated, but can be contaminated by the Lyman  $\alpha$  forest and we have been able to measure the sulphur column density only in four out of the seven DLAs under study.

In Table 2 we give our derived SII column densities and  $b$ -values. No sulphur abundance have been previously reported for the DLA systems under study. We now comment briefly the column density measurements of each DLA, starting with the two systems observed at higher spectral resolution (CASPEC data). For the ISIS data we first discuss those for which a determination of SII column density has been possible.

### 3.1. System at $z_{\text{abs}}=1.9730$ toward QSO 0013-004

For this absorber we derived the SII column density from the fit to the  $\lambda 1253 \text{ \AA}$  transition. The bluest transition at  $\lambda 1250 \text{ \AA}$  — the weakest one of the triplet — is quite noisy since it is located in the first order of the echellogram where the S/N ratio is low. The reddest transition at  $\lambda 1259 \text{ \AA}$  is completely blended, as one can see in Fig. 1a. We remark that the SII  $1253 \text{ \AA}$  line is found exactly at the same redshift ( $z_{\text{abs}}=1.9730$ ) as the ZnII and CrII absorptions studied by Pettini et al. (1994). The  $\lambda 1250 \text{ \AA}$  transition, in spite of the low S/N ratio, is very well matched by the synthetic spectrum built with this redshift value (solid line in Fig. 1a).

Our best fit to the SII  $1253 \text{ \AA}$  absorption gives  $\log N(\text{SII})=14.86$  and  $b=24.5 \text{ km s}^{-1}$ . The rest-frame

---

<sup>3</sup>The broadening parameter is defined as  $b = 2^{1/2}\sigma_v$ , where  $\sigma_v$  is the gaussian velocity dispersion for Doppler broadening.

equivalent width of the same line,  $EW_{\text{rest}} = 81 \text{ m}\text{\AA}$ , yields  $\log N(\text{SII}) = 14.74$  by using the linear part of the curve of growth (COG) which is indicative within the errors of a linear regime. In fact we obtained an acceptable fit to the SII 1253 absorption for a wide range of  $b$ -values, between  $b=14$  and  $b=35$  the extreme values and in both cases the resulting SII column density is consistent with the best fit value within the errors. We explored the uncertainty in the column density coming from the continuum tracing by shifting the continuum  $\pm 1 \text{ rms}$  and repeating the fit in each case. We obtained the best fits for  $\log N(\text{SII}) = 14.77$  ( $b=20.4$ ), and  $\log N(\text{SII}) = 14.91$  ( $b=24.6$ ) for the lower and upper continuum respectively. We adopt  $\log N(\text{SII}) = 14.86 (\pm 0.12)$  and  $b = 24.5 (\pm 10)$  given in Table 2, which takes into account the largest excursion of the SII column density values.

Unfortunately the SiII transitions available in our spectrum ( $\lambda\lambda 1260, 1304, \text{ and } 1526 \text{ \AA}$ ) are saturated or blended, making impossible a determination of the SiII column density for this system.

### 3.2. System at $z_{\text{abs}} = 2.0662$ toward QSO 2231-0015

Only SII 1253  $\text{\AA}$  absorption is available in this DLA, since the other two transitions of the triplet are contaminated by the Lyman  $\alpha$  forest (see upper panel of Fig. 1).

The fitted SII 1253  $\text{\AA}$  line is observed at the same redshift ( $z_{\text{abs}} = 2.0662$ ) as found by Lu et al. (1996) and PW99 in their study of this system. Moreover part of our wavelength range is also covered in the spectrum of PW99, and features in both spectra like OI 1302 and SII 1304 occur also at the same velocity position.

The SII absorption presents a high degree of saturation and only with an independent estimation of the  $b$ -value it would be possible to attain a reliable estimate of the SII column density. Unfortunately, no information is available on  $b$  value for this DLA, since abundances before this work have been obtained by using the opacity method. The NiII (1370  $\text{\AA}$ ) and CII (1335  $\text{\AA}$ ) absorptions observed in the higher S/N spectrum of PW99 are not detected in our spectrum making it impossible to constrain the  $b$  parameter in this system. We estimated  $\log N(\text{SII}) > 14.90$ , a lower limit obtained by using the rest-frame equivalent width and the linear part of the COG.

### 3.3. System at $z_{\text{abs}}=2.3745$ toward QSO 0841+129

This is the brightest target observed. The spectrum of this BL Lac object discovered by C. Hazard shows two DLAs previously analyzed by Pettini et al. (1997) and shown in Fig. 2a. Our best fit to the lower redshift damped absorption at  $z_{\text{abs}}=2.374$  gives  $\log N(\text{HI}) = 20.96 \pm 0.10$  in perfect agreement with  $\log N(\text{HI})=20.95 \pm 0.10$  reported by Pettini et al. (1997).

For this  $z_{\text{abs}}=2.3745$  system a feature at  $4 \sigma$  significance level is observed at the expected redshifted position of the strongest triplet transition SII 1259 Å (vertical arrow in Fig. 2b). The blue ISIS spectrum of Pettini et al. (1997; see their Fig. 1) recorded at about half of our resolution also shows this feature indicating that it is real.

The SII 1259 Å transition is observed in the red wing of the higher redshift damped Ly  $\alpha$  absorption at  $z_{\text{abs}}=2.476$ , which unfortunately precludes the detection of the other two bluer absorptions of the SII triplet. Our best fit to this damped absorption ( $z_{\text{abs}}=2.476$ ) shown with solid and dotted lines in Fig. 2a,b gives  $\log N(\text{HI})= 20.83 \pm 0.10$  in good agreement with  $\log N(\text{HI})=20.79 \pm 0.10$  reported by Pettini et al. (1997). We re-normalized this portion of the spectrum to the Ly  $\alpha$  profile before fitting the SII line. For this system there is not independent information on the  $b$ -value from the literature. In order to constrain the SII column density we estimated the  $b$ - value in this line of sight from the analysis of the FeII  $\lambda\lambda$  1121, 1125, 1127,1133,1143,1144 Å transitions. We obtained  $\log N(\text{FeII})=14.83 \pm 0.15$  and  $b=20 \pm 3 \text{ km s}^{-1}$  (see Fig. 2c). The errors in the FeII column density and  $b$ -value take into account the fit errors and in the error due to the uncertainty of the continuum placement.

By fixing  $b(\text{SII})=b(\text{FeII})= 20 \text{ km s}^{-1}$  and  $z_{\text{abs}}=2.3745$  — at which we observe 6 FeII absorptions — in the SII fitting procedure we obtained  $\log N(\text{SII}) = 14.92 \pm 0.09$ . In Fig. 3a this fit is shown with a solid line overimposed to the spectrum re-normalized to the Ly $\alpha$  absorption. Changing the  $b$ -value by  $\pm 3 \text{ km s}^{-1}$  affects the SII column density only by  $\leq 0.02 \text{ dex}$ . Moreover if we use  $b=13 \text{ km s}^{-1}$  obtained from the analysis of the NI 1134 Å and 1200 Å multiplets we obtain  $\log N(\text{SII}) = 14.89 \pm 0.14$  still consistent with the column density obtained for  $b=20 \text{ km s}^{-1}$ . These results clearly indicate that the SII absorption under study is unsaturated and this is reinforced by the fact that by using the rest equivalent width ( $\text{EW}_{\text{rest}} = 175 \text{ mÅ}$ ) over the linear part of the COG we obtained again  $\log N(\text{SII}) = 14.89$ . We estimated the error due to the continuum placement by fitting the SII absorption in the spectra normalized to the local continua shown with dotted lines in Fig. 2a, and we obtained  $\epsilon_{\log N(\text{SII})} = \begin{smallmatrix} +0.16 \\ -0.21 \end{smallmatrix}$ . This error dominates the error budget and we adopted  $\log N(\text{SII}) = 14.92 \begin{smallmatrix} +0.16 \\ -0.21 \end{smallmatrix}$ . We remark that in case we consider the SII absorption



non detected, we can use  $\log N(\text{SII}) < 14.92$  as a conservative  $4\sigma$  upper limit. Even in this case the result would not affect the main conclusion of the present work, as we discuss in Section 4. Nevertheless as it has been explained above there are at least three good reasons which make this detection reliable: i) the feature seems to be also present in the spectrum of Pettini et al. 1997, ii) the feature is observed at  $z_{\text{abs}}=2.3745$  the same redshift at which we observed six single-component transitions of FeII shown in Fig. 2c, iii) the single component-structure and the redshift are confirmed by the absorptions of SII 1808, CrII 2056,2062,2066, ZnII2062 observed in the higher resolution and S/N HIRES-Keck spectrum of PW99.

### 3.4. System at $z_{\text{abs}}=2.4762$ toward QSO 0841+129

As can be seen in Fig. 2a,b the SII triplet of this system is overimposed to a smooth, broad absorption which is also seen in the spectrum of Pettini et al. (1997). We investigated the possibility that this broad absorption may be due to Ly $\alpha$  line-locking with the velocity separation of CIV or SiIV resonance doublets since this process is associated with absorption systems at  $z_{\text{abs}} \simeq z_{\text{em}}$  of the QSO (Srianand, 1999). This is the case here since  $z_{\text{em}} \simeq 2.5$  have been estimated from the onset of Ly  $\alpha$  forest (Pettini et al. 1997). However, from the line-locking process one would expect a velocity separation between the broad profile and the  $z_{\text{abs}}=2.4762$  Ly $\alpha$  absorptions correspondent to the velocity separation between the two lines of the CIV or SiIV doublet of that system. This is not the case here, at least for the CIV or SiIV doublets. In any case, the presence of the broad feature does not affect our measurements because the SII absorptions are thin, as expected for DLA metal lines, and are clearly seen distinguishable from the broad feature. In order to analyze the SII triplet we renormalized this portion of the spectrum to the broad profile shown in Fig. 2b. The SII 1253 Å transition is heavily blended and we excluded this feature from the fitting procedure. Our best fit to the SII 1250 Å and 1259 Å transitions gives  $\log N(\text{SII}) = 14.81$ ,  $b=13.5 \text{ km s}^{-1}$  and  $z_{\text{abs}}=2.4762$ . In Fig. 3b we show the synthetic spectrum of the SII triplet computed with these parameters. We remark that redshift obtained from the SII triplet is in perfect agreement with the one found by PW99 for different single-component metal absorptions observed in their Keck spectrum, and hence enhancing the reliability of the SII detections. Pettini et al. 1999 gave  $z_{\text{abs}}=2.4764$  for this system but it was obtained just from the fit to the wide damped Lyman  $\alpha$  absorption.

By using the rest equivalent width ( $\text{EW}_{\text{rest}} = 48 \text{ mÅ}$ ) of the weakest 1250 Å transition over the linear part of the COG we obtained essentially the same column density  $\log N(\text{SII}) = 14.80$  indicating that this transition is not saturated. Again the major uncertainty in the column density comes from the continuum

placement. We renormalized the spectra to the upper and lower continua shown with dotted lines in Fig. 2b and we measured for SII 1250 Å absorption  $EW_{\text{rest}} = 70$  and  $30 \text{ mÅ}$  which yield  $\log N(\text{SII}) = 14.96$  and  $14.60 \text{ atoms/cm}^{-2}$  respectively. We adopted  $\log N(\text{SII}) = 14.81_{-0.21}^{+0.15}$  given in Table 2.

### 3.5. System at $z_{\text{abs}} = 1.999$ toward QSO 1215+333

Also in this system the SII triplet is observed overimposed on a wide absorption (see Fig. 2d). In this case an origin in the line-locking process is unlikely because there is a significant difference between  $z_{\text{abs}}$  and  $z_{\text{em}}$  (see Table 1). To analyse the SII triplet we have renormalized this portion of the spectrum to the broad absorption (Fig. 3c). The SII 1253 Å transition though partially blended is the only feature that can be used to derive the column density.

The SII 1259 Å transition is heavily blended and our best fit to the SII 1253 Å line gives  $\log N(\text{SII}) = 15.11$  for  $b = 55 \text{ km s}^{-1}$ . A synthetic SII spectrum built with these values is shown with a solid line overimposed to the observed spectrum in Fig. 3c. In order to explore the degree of saturation of this absorption we performed the fit for a large range of  $b$  values. We obtained  $b = 70 \text{ km s}^{-1}$  ( $\log N(\text{SII}) = 14.99$ ) and  $b = 18 \text{ km s}^{-1}$  ( $\log N(\text{SII}) = 15.23$ ) the maximum and minimum  $b$  values which can give an acceptable fit to the observed profile. Again, the column density does not depend very much on the  $b$ -value, indicating a low degree of saturation. In fact the SII 1253  $EW_{\text{rest}} = 0.150 \text{ Å}$  gives  $\log N(\text{SII}) = 14.99$  over the linear part of the COG. Also in this case the major source of uncertainty in the column density comes from the continuum placement. In order to estimate this error we re-normalized the spectrum to the continuum positions shown with dotted lines in Fig. 2d. With the upper continuum we obtained a minimum  $b = 15 \text{ km s}^{-1}$  for which an acceptable fit can be obtained, yielding  $\log N(\text{SII}) = 15.36$ . In this case the 1253 line presents a certain degree of saturation since the rest equivalent width over the linear part of the COG gives  $\log N(\text{SII}) = 15.10$ . For the lower continuum the column density does not depend on the  $b$ -value and we obtained  $\log N(\text{SII}) = 15.00 \pm 0.02$  for  $18 \leq b \leq 50 \text{ km s}^{-1}$ . We obtain therefore for this system  $\log N(\text{SII}) = 15.11_{-0.12}^{+0.25}$ . Nevertheless, since this determination relies on just one absorption which is partially blended and no other single metal absorptions are available in our spectrum to confirm the redshift, we adopt the most conservative result by considering the sulphur abundance as an upper limit  $\log N(\text{SII}) < 15.11 + 0.25$ , and we remark that this does not change the main conclusion of this work, as discussed in Section 4.

### 3.6. System at $z_{\text{abs}}=2.1408$ toward QSO 0149+335

None of the three absorptions of the SII triplet are detected. Their expected redshifted positions are marked with dashed vertical lines in Fig.3d. The low signal-to-noise ratio in this spectral range ( $S/N \simeq 6$ ) yields a poor stringent upper limit on the SII column density and hence on the abundance of this element (see Table 2 and Table 3.)

### 3.7. System at $z_{\text{abs}}= 2.4658$ toward QSO 1223+178

In Fig. 3e we show the SII portion of the spectrum already normalized to the broad absorption. The vertical dashed lines show the expected positions of the triplet. The SII 1253 Å line if present is contaminated by a cosmic ray, and the SII 1259 Å, if present, is heavily blended with a Ly $\alpha$  interloper. The weakest 1250 Å absorption seems undetected in our  $S/N \simeq 7$  spectrum. If this is the case we obtain  $\log N(\text{SII}) < 15.18$  and an upper limit  $[S/Zn] \leq -0.01$  by using the ZnII column density given by Pettini et al. (1994). However the poor quality of the spectrum in the SII region and the difficulty in positioning the continuum precludes a reliable analysis of the SII triplet in this system and for that reason we have omitted this DLA from the rest of the present study.

## 4. Discussion

### 4.1. Abundances of $\alpha$ and iron-peak elements

In Table 3 we list the abundances of the iron-peak elements Fe, Zn and Cr as well as the abundances of the  $\alpha$  elements S and Si for the DLA systems under investigation.

Iron-peak elements are produced in nuclear statistical equilibrium and are expected to trace each other in the course of chemical evolution. Observations of metal-poor stars in the Galaxy confirm that Cr and Zn follow closely Fe in essentially solar proportions down to very low metallicities, although Cr deviates from this behaviour becoming slightly underabundant compared to iron at about  $[\text{Fe}/\text{H}] \leq -2$  (Ryan et al. 1996; Sneden, Gratton & Crocker 1991)

DLA systems, which have metallicities  $[\text{Zn}/\text{H}] > -2$ , show instead systematic differences among the iron-peak elements, with Zn more abundant than Cr and Fe. Abundances of these elements in the DLAs under study are also given in Table 3. The systematic difference between Zn and Cr is attributed to

differential depletion of these two elements from the gas phase to dust grains (Pettini et al. 1994, 1997). In fact, enhanced  $[Zn/Cr]$  and  $[Zn/Fe]$  ratios are observed also in the nearby interstellar medium, which is expected to have solar chemical composition, and are attributed to differential dust depletion, being Zn almost undepleted (Roth & Blades 1995, Savage & Sembach 1996).

The presence of dust depletion may also affect the analysis of some  $\alpha$ -elements such as silicon. Silicon is the  $\alpha$  element with the largest number of measurements in DLA systems (Lu et al. 1996, PW99), however can be depleted up to 1 order of magnitude in the Galactic interstellar medium (Savage & Sembach 1996). Sulphur also shows in Galactic metal-poor stars the typical enhancement of  $\alpha$ -elements with  $[S/Fe] \simeq +0.4/+0.6$  (Francois 1988), but contrary to Si, sulphur is undepleted from gas to dust.

The fact that typical depletions of S and Zn in Galactic interstellar clouds are in the ranges  $[-0.05, 0.0]$  and  $[-0.25, -0.13]$  dex respectively (Savage & Sembach 1996; Roth & Blades 1995), makes the  $[S/Zn]$  ratio a reliable dust-free diagnostic tool of the  $[\alpha/\text{iron-peak}]$  abundance ratio in DLAs.

In Table 4 we compile all the extant  $[S/Zn]$  measurements in DLA systems. For the sake of comparison we also give, when available, the  $[Si/Fe]$  ratios for these DLAs. One can see that while the  $[Si/Fe]$  ratios emulate the typical halo-like abundance pattern ( $[\alpha/Fe] \simeq +0.5$ ), the  $[S/Zn]$  ratios do not show evidence for  $\alpha/Fe$  enhancement. Following Vladilo (1998) we have corrected, when possible <sup>4</sup>, the observed  $[Si/Fe]$  ratios from dust effects. These values are also reported in Table 4, and show that, when dust correction is quantitatively taken into account, the corrected ratios,  $[Si/Fe]_{corr}$  have lower values similar to the  $[S/Zn]$  ratios. This result confirms that dust plays an important role in the observed  $[Si/Fe]$  overabundance and suggests that the assumptions adopted in the dust correction method seem to be appropriate for DLAs.

The  $z_{abs}=1.973$  DLA system toward Q0013-004 included in our sample is one of the few DLAs for which molecular hydrogen has been detected (Ge & Betchold 1997). The presence of molecular gas is indicative of an environment hospitable to grains and we should expect a large depletion of refractory elements. This is indeed confirmed by the much higher abundance of Zn compared to Fe (Table 3). In a dust-rich DLA Zn can be expected to be somewhat depleted — in a higher proportion than S as it occurs in the galactic ISM — and a slight enhancement of the  $[S/Zn]$  ratio could be expected. In order to quantify this effect we corrected the ratio  $[S/Zn]_{obs}=-0.39$  measured in this system following Vladilo (1998) and we obtained  $[S/Zn]_{corr} = -0.41$ . The difference is very small and lower than the typical measurement errors,

---

<sup>4</sup>For DLAs with available abundances of both Fe and Zn

supporting the assumption that the S/Zn ratio is a reliable indicator of the  $\alpha$ /iron-peak ratios in DLAs also in the presence of a significant amount of dust.

Besides the problem of differential depletion, the ionization balance could also affect the measurement of the elemental abundance ratios as discussed recently by Howk & Savage (1999). From the presence of Al III at the same radial velocity of low ions in DLA systems, these authors argue that ionization effects can also produce an apparent enhancement of the [Si/Fe] ratios measured just from Si II and Fe II lines (i.e. from only one ionization state). Dust or ionization effects are both therefore going in the direction of producing an enhancement of the Si/Fe. However, from an analysis of literature data we do not find evidence for a relative [Si/Fe] enhancement at the highest values of the ionization ratio Al III/Al II in the 5 DLA systems with available measurements of Al II, Al III, Si II and Fe II column densities.

In a separate work we show that the presence of ionized gas surrounding the HI regions in DLA systems should affect only marginally the relative abundances measured from low ions (Vladilo et al., in preparation).

#### 4.2. Implications for solar $\alpha$ /Fe ratios

In the early stages of the chemical evolution of galaxies the abundances are dominated by Type II SNe products, richer in  $\alpha$ -elements yielding an enhancement of the  $\alpha$  elements over iron-peak elements. At later stages of evolution the contribution of Type Ia SNe, richer in iron-peak elements, reduces the [ $\alpha$ /Fe-peak] ratio. The precise timing in which the products of Type Ia SNe become important depends on the star formation rate and on the initial mass function. The [ $\alpha$ /Fe] ratio is therefore a primary indicator of the type of chemical evolution and can be used to understand the nature of DLA galaxies.

In Fig. 4 we show the [S/Zn] measurements in DLA galaxies. Our sulphur abundances are represented by squares which also include the DLAs at  $z_{\text{abs}}=2.309$  towards QSO 0100+1300 (PHL 957) and  $z_{\text{abs}}=3.025$  towards QSO 0347–3819 discussed in MCV98. Triangles represent sulphur abundances from literature (see Table 4 for references). For the sake of comparison we also show in the figure the [S/Fe] ratios measured in Galactic metal-poor stars by Francois (1987,1988), with star symbols, and by Clegg et al. (1981), with asterisks.

Even at first glance it is clear that the [S/Zn] ratios in DLAs do not show the  $\alpha$ -enhancement seen in Galactic metal-poor stars and that are located in a different sector of the diagramme. This result, already

advanced in MCV98, is now rather firm since it is based on 6 new measurements of DLA systems which sample a wide range of metallicities. The 4 limits but one shown in Fig. 4, are also consistent with this result. The exception is the system at  $z_{\text{abs}}=2.476$  towards Q0841+129 giving  $[\text{S}/\text{Zn}]>0.2$ , which is therefore consistent with an intrinsic  $\alpha$ -enhancement. The above results are robust against a possible contamination of the sulphur absorptions by the Lyman  $\alpha$  forest. Should the Lyman  $\alpha$  forest contaminate some of the detected SII features, the real  $[\text{S}/\text{Zn}]$  would be even lower and this would reinforce the result.

The  $[\text{S}/\text{Zn}]$  ratios in DLA systems are significantly lower than the Galactic ones at comparable metallicities and suggest that DLA galaxies have undergone a different chemical evolution from that of the Milky-Way. The frequently adopted hypothesis that DLAs are progenitors of the spiral galaxies, apparently supported by the observed  $[\text{Si}/\text{Fe}]$  ratios, is not confirmed when a dust-free diagnostic as  $[\text{S}/\text{Zn}]$  is considered. Results based on  $[\text{Si}/\text{Fe}]$  measurements should be treated with caution, unless dust depletion is properly taken into account.

Some of the  $[\text{S}/\text{Zn}]$  ratios, far from showing an enhancement respect to the solar value, show instead negative values. These cases happen at the highest values of metallicity in our sample, while the highest  $[\text{S}/\text{Zn}]$  values are observed at the lowest metallicities. In particular the lower limit suggestive of intrinsic enhancement ( $z_{\text{abs}}=2.476$  in Q0841+129) is found at the lowest value of  $[\text{Zn}/\text{H}]$  in our sample. Therefore, the  $[\text{S}/\text{Zn}]$  abundances in DLAs are consistent with a general trend of decreasing ratio with increasing metallicity. The limited amount of data are insufficient to firmly establish the presence of a correlation, which only can be considered with the present data if we use the  $[\text{S}/\text{Zn}]$  values in DLAs at  $z_{\text{abs}}= 2.374$  towards QSO 0841+129 as a measurement and not as an upper limit. In that case a linear regression to the data yields a correlation coefficient of  $r=-0.77$ , obtained only with 5 data points (see Fig. 4). If confirmed by a larger data sample the trend would be the first observational evidence of the expected decrease of the  $\alpha/\text{Fe}$  ratio in DLAs during the course of chemical evolution. At variance with what observed in our Galaxy, however, the  $\alpha/\text{iron-peak}$  ratio attains solar values at low metallicity ( $[\text{Fe}/\text{H}] \approx -1$ ) and decrease further at higher metallicities. This trend is the one predicted by chemical evolution models of galaxies with a low star formation rate (Matteucci et al. 1997) and, if confirmed by future observations, it would have an important implication on the origin of DLA systems. Chemical evolutionary models predict  $[\alpha/\text{Fe}]\simeq 0$  at low metallicities, ( $[\text{Fe}/\text{H}] \leq -1$ ) when star formation proceeds in bursts separated by quiescent periods, as happens in dwarf galaxies, and when star formation is not as fast as in our Galaxy, as it happens in LSB galaxies and in the outer regions of disks (Jiménez et al. 1999). In these galaxies the metal enrichment is so slow that Type Ia supernovae have enough time to evolve and enrich the medium with iron-peak elements,

in such a way as to balance the  $\alpha$ -elements previously produced by Type II supernovae, when the overall metallicity is still low. In any case by considering the sulphur abundance in DLAs at  $z_{\text{abs}}=2.374$  towards QSO 0841+129 an upper limit we may still conclude that the [S/Zn] ratios in DLAs are markedly different from those observed in our Galaxy at comparable metallicities, implying a different chemical history.

In Fig. 5 the [S/Zn] are plotted versus the absorber redshift  $z_{\text{abs}}$ . Chemical evolution effects should in general decrease the [S/Zn] with cosmic time and one would expect a positive trend with  $z_{\text{abs}}$ . Our sample, however, does not show such a correlation. Pettini et al. (1997, 1999) do not find either any trend of the [Zn/H] ratio with  $z_{\text{abs}}$ , contrary to the expectation of a general increase of metallicity with cosmic time. A significant spread of [Zn/H] abundances at a given redshift is expected when different formation redshifts or spatial gradients are considered in modeling the intervening galaxies (Jiménez et al. 1998). Thus, different epoch of formation and different regions within a galaxy could be responsible also for the lack of correlation between the [S/Zn] ratios and redshift. The fact that we possibly detect a trend with [Zn/H], but not with  $z_{\text{abs}}$ , suggests that metallicity is a better indicator of evolution since, contrary to redshift, it is independent of the epoch of formation of the individual galaxies. We do not exclude however that evolution with redshift can be detected when the data will have a better redshift coverage.

It is worth mentioning that also in the Milky Way there are some measurements of [ $\alpha$ /Fe-peak] ratios not enhanced at low metallicity. These cases are found among halo dwarfs, but are extremely rare. Carney et al. (1997) found [Mg/Fe] = -0.31 in the star BD +80 245, while Nissen & Schuster (1997) found [Mg/Fe] ratios ranging from -0.1 to 0.2 in their stars. These stars are all characterized by large apogalactic distances and the unusual abundance ratios have been interpreted as the chemical signature of a merger or accretion events. The stars before the merging or accretion process are thought to belong to a satellite galaxy which experienced a different chemical evolution history than the Milky Way. The presence of these cases do not imply therefore a connection between what we observe in DLA galaxies and the typical behaviour of Milky Way chemical evolution.

We remark that also the nitrogen abundances in DLAs do not seem to follow the behaviour of Galactic metal-poor stars when dust free ([N/S]), or dust-corrected ([N/Fe<sub>corr</sub>]) ratios are used to determine the nitrogen relative abundances (Lu, Sargent, & Barlow 1998; Centurión et al. 1998).

We conclude that the DLA galaxies do not show the abundance properties usually expected for the progenitors, of a spiral galaxy as the Milky Way. The unusual abundance ratios suggest that the DLA galaxies are objects with low, or episodic, star formation rates such as LSB or dwarf galaxies. Part of the

DLAs may be proto-spirals, for which the line of sight samples the outer regions, which are known to have a slower evolution than the internal regions of the disks.

These indications on the nature of DLA systems based on chemical abundances are in agreement with the results based on imaging studies at low redshifts, where the candidates DLA galaxies show a variety of morphological types including dwarfs and LSBs, while spirals are not the dominant contributors (Le Brun et al. 1997, Rao & Turnshek 1998). Nevertheless, it is important to remark that the spectroscopic sample of DLA systems is probably biased against detection of spirals, since high column density clouds located in environments with relatively high metallicity and dust can be missed owing to obscuration of the background QSO (Pei et al. 1991, Vladilo 1999).



## REFERENCES

- Anders, E., & Grevesse, N. 1989, *Geochim. Cosmochim. Acta*, 53, 197
- Carney, B.W., Wright, J.S., Sneden, C., Laird, J.B., Aguilar, L.A., Latham, D.W. 1997, *AJ*114, 363
- Centurión, M., Bonifacio, P., Molaro, P., Vladilo, G. 1998, *ApJ*, 509, 620
- Clegg, R.E.S., Lambert, D.L. & Tomkin, J. 1981, *ApJ*, 250, 262
- Fan, X.M., & Tytler, D. 1994, *ApJS*, 94, 17
- Fontana, A. & Ballester, P. 1995, *The Messenger*, 80,37
- Francoise, P. 1987, *A&A*, 176, 294
- Francoise, P. 1988, *A&A*, 195, 226
- Ge, J. & Betchtold, J. 1997, *ApJ*, 477, 73
- Haehnelt, M.G., Steinmetz, M. & Rauch, M. 1998, *ApJ*, 495, 647
- Howk, J.C. & Savage, K.R. 1999, *ApJ*, in press (astro-ph/9907428)
- Jimenez, R., Bowen, D.V., & Matteucci, F. 1999, *ApJ*, 514, 83
- Jimenez, R., Padoan, P., Matteucci, F., & Heavens, A.F. 1998, *MNRAS*, 299, 123
- Kulkarni, V.P., Huang, K., Green, R.F., Bechtold, J., Welty, D.E., York, D.G. 1996, *MNRAS*, 279, 197
- Ledoux, C., Petitjean, P., Bergeron, J., Wampler, E.J., & Srianand R. 1998, *A&A*, 337, 51
- Le Brun, V., Bergeron, J., Boisse, P., & Deharveng, J.M. 1997, *A&A*, 321, 733
- Lu, L., Sargent, W.L.W., & Barlow, T.A. 1998, *AJ*, 115, 55
- Lu, L., Sargent, W.L.W., Barlow, T.A., Churchill, C.W., Vogt, S. 1996, *ApJS*, 107, 475
- Lu, L., Savage, B.D., Tripp, T.M., & Meyer, D.M. 1995, *ApJ*, 477, 597
- Matteucci, F., Molaro, P., & Vladilo, G. 1997, *A&A*, 321, 45

- Molaro, P., Centuri3n, M., & Vladilo, G. 1998, MNRAS, 293, L37 (MCV98)
- Molaro, P., D’odorico, S., Fontana, A., Savaglio, S., Vladilo, G. 1996, A&A308, 1
- Morton, D.C. 1991, ApJS, 77, 119
- Nissen, P.E., & Schuster, W.J. 1997 A&A, 1997, 326, 751
- Pei, Y.C., Fall, S.M., & Bechtold, J. 1991, ApJ, 378, 6
- Pettini, M., King, D.L., Smith, L.J., Hunstead, R.W. 1997b, ApJ, 478, 536
- Pettini, M., Smith, L.J., Hunstead, R.W., King, D.L. 1994, ApJ, 426, 79
- Pettini, M., Ellison, S.L., Steidel, C.C., Bowen, D.V. 1999, ApJ, 510, 576
- Pettini, M., Smith, L.J., King, D.L., Hunstead, R.W. 1997, ApJ, 486, 665
- Prochaska, J.X. & Wolfe, A.M. 1997, ApJ, 487, 73
- Prochaska, J.X. & Wolfe, A.M. 1999, ApJS, 121, 369 (PW99)
- Ryan, S.G., Norris, J.E., & Beers, T.C. 1996, ApJ, 471,254
- Rao, S.M., & Turnshek, D.A. 1998, ApJ, 500, L115
- Roth, K.C., & Blades, J.C. 1995, ApJ, 445, 95
- Savage, B.D., & Sembach, K.R. 1996, Ann. Rev. Astron. Astrophys., 34, 279
- Snedden, C., Gratton, R., & Crocker, D.A. 1991, A&A, 246, 354
- Srianand, R. 1999, ApJ, in press (astro-ph/9908179)
- Vladilo, G., 1998, ApJ, 493, 583
- Vladilo, G., 1999, in *The Evolution of Galaxies on Cosmological Timescales* ASP Conference Series, eds. J.E. Beckman, and T.J. Mahoney (astro-ph/9903406).
- Wolfe, A.M., Lanzetta, K.M., Foltz, C.B., Chaffee, F.H. 1995, ApJ, 454, 698

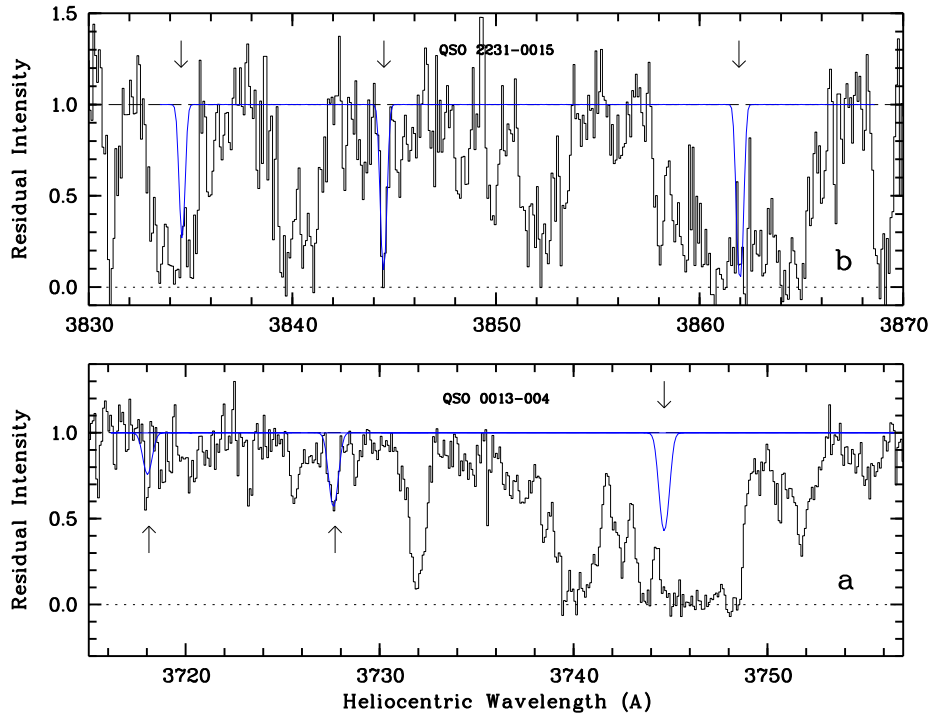
Fig. 1.— SII triplet of  $z_{abs}=1.9731$  and  $z_{abs}=2.0662$  DLA systems observed in the CASPEC normalized spectra of QSO 0013-004 and QSO 2231-0015, respectively. Smooth lines: synthetic spectra obtained from the fit of the  $\lambda 1253 \text{ \AA}$  transition of the SII triplet (see text for details).

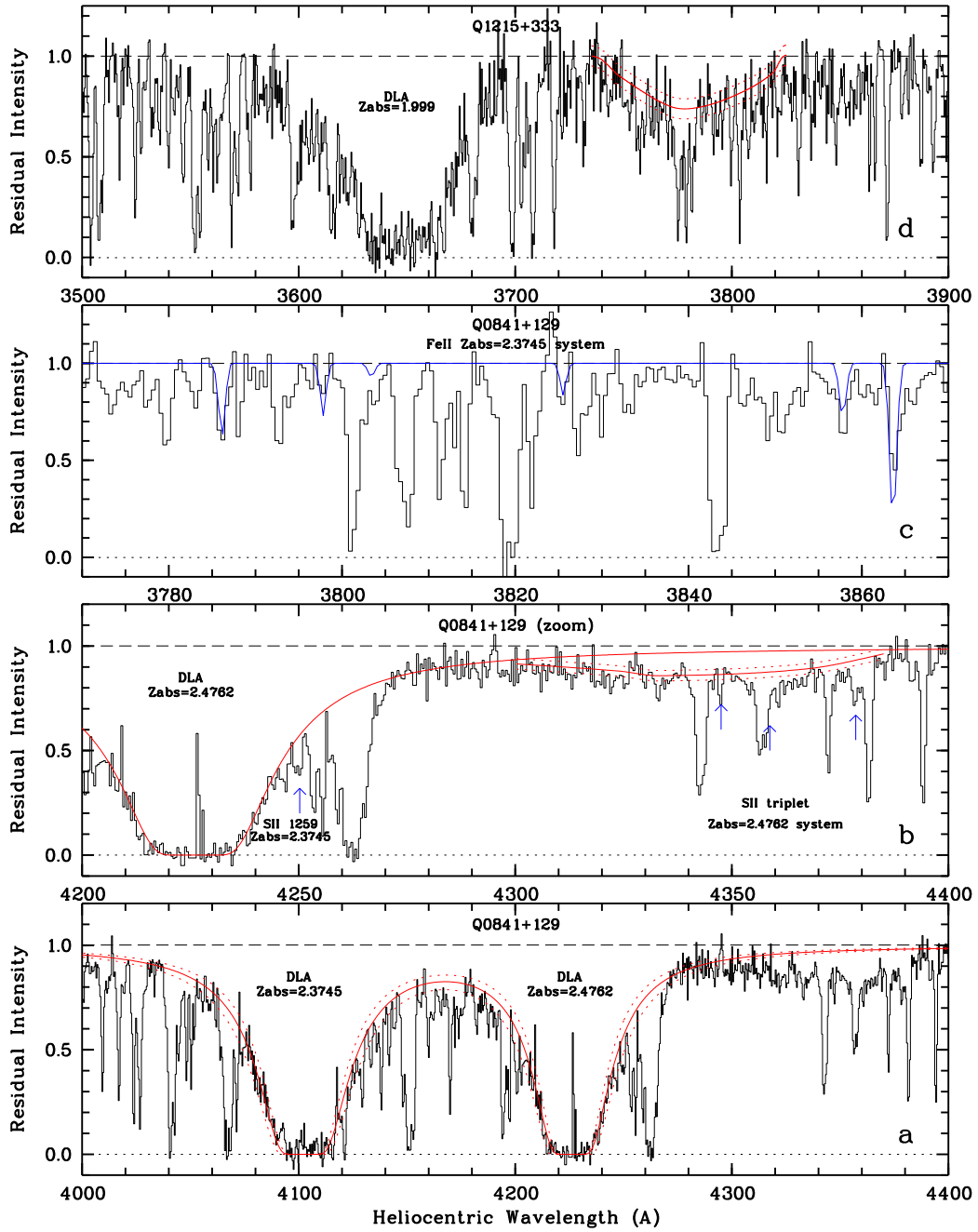
Fig. 2.— Normalized portions of the ISIS blue spectra of QSO 0841+129 and QSO 1215+333. (a) The two DLA systems towards QSO 0841+129. Solid and dotted lines show the synthetic damping profiles corresponding to the column density of neutral hydrogen given in Table 1. (b) SII 1259  $\text{\AA}$  transition of  $z_{abs}=2.3745$  DLA system, and SII triplet of DLA at  $z_{abs}=2.4762$  towards QSO 0841+129. The left single arrow indicates the position of SII 1259 at  $z_{abs}=2.3745$  obtained from the six FeII absorptions and in perfect agreement with the value given by PW99. The three arrows in the right side are plotted at the redshifted position of the SII triplet for the DLA system at  $z_{abs}=2.4762$ . Solid and dotted lines show the damped profile and the continua to which this portion of the spectra have been re-normalized in order to measure the SII column densities in both DLA systems. (c) FeII lines of  $z_{abs}=2.3745$  DLA system in the normalized spectrum of QSO 0841+129. Solid lines show the synthetic spectrum obtained from the fit of all the FeII absorptions contemporaneously. (d) Normalized portion of QSO 1215+333 spectrum in the region of the DLA absorption and SII triplet. The solid and dotted lines are the continua to which the spectrum have been re-normalized in order to analyzed the SII absorptions.

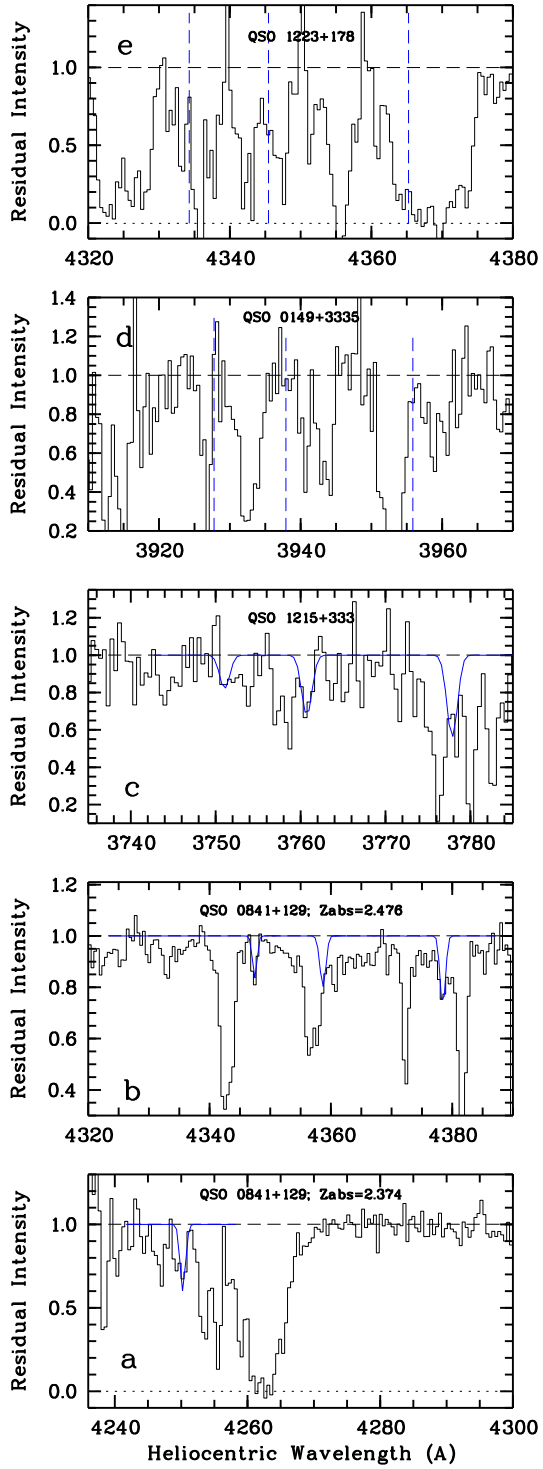
Fig. 3.— Normalized blue ISIS spectra of the QSOs in our sample centered in the SII triplet region. The solid lines are the synthetic SII spectra resulting from the best fits to the observed profiles. Dashed vertical lines in panels d) and e) indicate the expected positions of the undetected SII triplet.

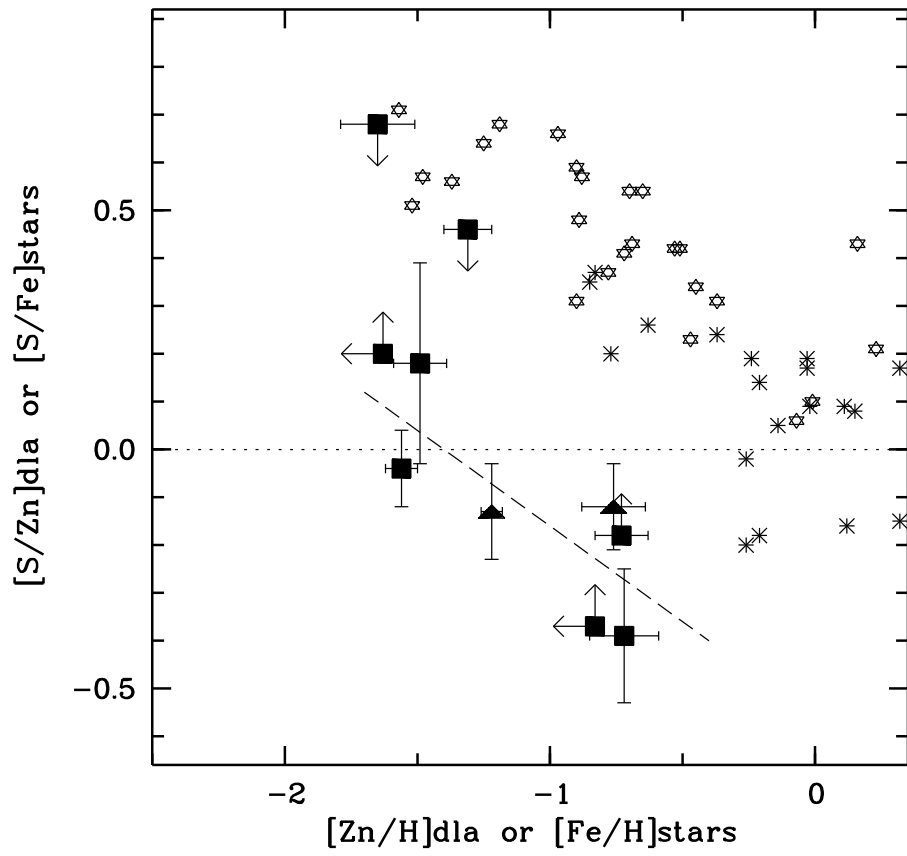
Fig. 4.— Measurements of  $[S/Zn]$  ratio in DLA systems. **Squares:** Sulphur abundance determinations obtained by our group including  $z_{abs}=2.309$  towards QSO 0100+1300 and  $z_{abs}=3.025$  towards QSO 0347–3819 given in MCV98. Zinc abundances are from the literature (see references in Table 2). **Triangles:** Sulphur and Zinc abundances determinations from the literature (see references in Table 4). **Stars and asterisks:**  $[S/Fe]$  ratio measured in Galactic stars by Francoise 1987, 1988 and Clegg et al. 1981 respectively. **Dashed line:** Result of a linear regression of  $[S/Zn]$  versus  $[Zn/H]$  measurements in DLA systems including as measurements  $z_{abs}=2.374$  towards QSO0841+129. Limits are not included in the correlation analysis.

Fig. 5.— The  $[S/Zn]$  abundance ratios in DLAs plotted versus metallicity  $[Zn/H]$









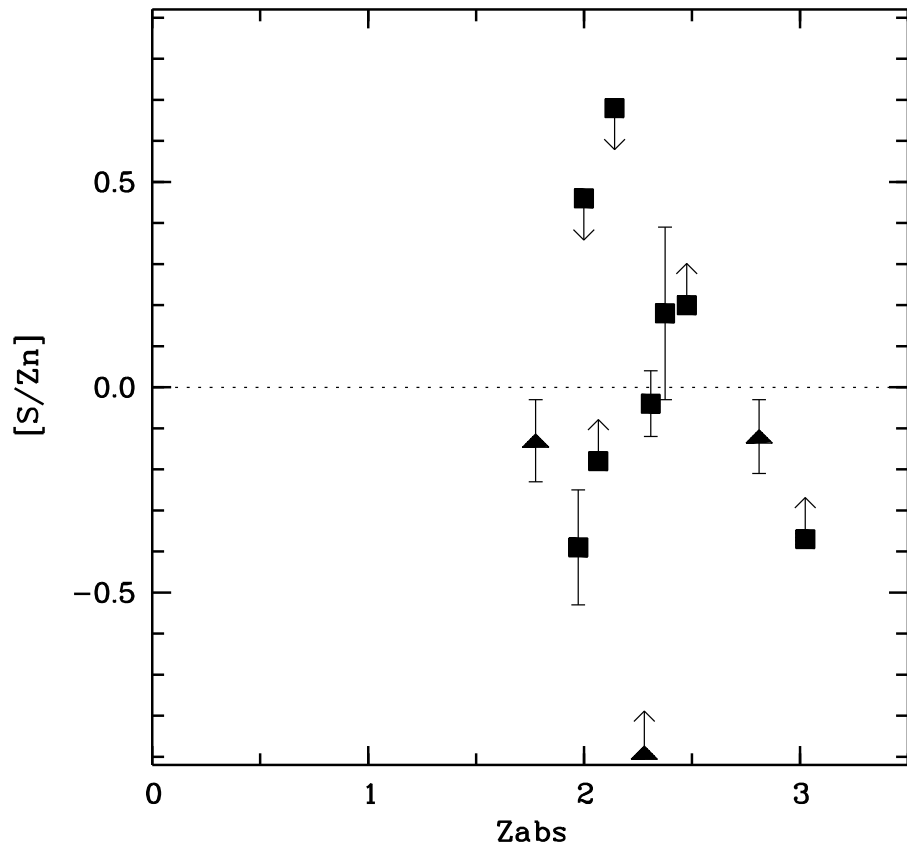




Table 1. Journal of observations

QSO	V	$z_{\text{em}}$	$z_{\text{abs}}$	Telescope	Date	$t_{\text{exp}}$ (s)	No. spectra	Coverage ( $\text{\AA}$ )
0013–004	18.2	2.084	1.9730	ESO 3.6m	1997 Sep 4	13500	2	3661-4638
					1997 Sep 5	14400	2	
					1997 Sep 6	14400	2	
0149+335	18.5	2.431	2.1408	WHT	1998 Dec 21	3600	2	3431-4366
0841+129	17.0	2.5:	2.3745	WHT	1998 Dec 21	3600	2	3710-4643
			2.4762	WHT	1998 Dec 23	4000	2	3710-4643
1215+333	17.5	2.606	1.999	WHT	1998 Dec 22	3560	2	3350-4190
					1998 Dec 24	3600	2	
1223+178	18.1	2.936	2.4658	WHT	1998 Dec 24	3600	2	3880-4775
2231–0015	17.4	3.020	2.0662	ESO 3.6m	1997 Sep 5	7200	1	3661-4638
					1997 Sep 6	7200	1	

Table 2. Column densities.

QSO	$z_{\text{abs}}$	$\log N(\text{SII})$	b	ref	$\log N(\text{ZnII})$	ref	$\log N(\text{HI})$	ref
0013-004	1.9730	$14.86 \pm 0.12$	$24.5 \pm 10$	1	$12.63 \pm 0.06$	2	$20.70 \pm 0.05$	3
0149+3335	2.1408	$\leq 14.80$	...	1	$11.50 \pm 0.10$	4	$20.50 \pm 0.10$	4
0841+129	2.3745	$14.92^{+0.16}_{-0.21}$	$20 \pm 3^{\text{a}}$	1	$12.12 \pm 0.05$	4	$20.96 \pm 0.10$	1
0841+129	2.4762	$14.81 \pm 0.21$	$13.5 \pm 2$	1	$< 11.78$	4	$20.76 \pm 0.10$	1
1215+333	1.999	$< 15.36$	18-70	1	$12.29 \pm 0.06$	4	$20.95 \pm 0.07$	2
2231-0015	2.0662	$> 14.90$	<sup>b</sup>	1	$12.46 \pm 0.02$	4	$20.56 \pm 0.10$	4

<sup>a</sup>From the fit to the FeII transtions 1121,1125,1127,1133,1143,1144Å

<sup>b</sup>Limit obtained by using the linear part of the COG, since no information is available on b value, (see text for details)

REFERENCES — (1) This paper; (2) Pettini et al. (1994); (3) Ge & Betchold (1997); (4) Prochaska & Wolfe 1999

Table 3. Abundances of  $\alpha$  elements and iron-peak elements

QSO	$z_{\text{abs}}$	[S/H] <sup>a</sup>	[Si/H] <sup>b</sup>	[Fe/H]	[Cr/H]	[Zn/H]	Refs. <sup>c</sup>
0013–004	1.973	$-1.11 \pm 0.14$	...	$-1.84 \pm 0.05$	$\leq -1.68$	$-0.72 \pm 0.13$	(1,2,2)
0149+3335	2.141	$\leq -0.97$	$-1.68 \pm 0.11$	$-1.81 \pm 0.10$	$-1.37 \pm 0.11$	$-1.65 \pm 0.14$	(3,3,3)
0841+129	2.374	$-1.31^{+0.19}_{-0.23}$	$-1.27 \pm 0.09$	$-1.64 \pm 0.17$	$-1.56 \pm 0.10$	$-1.49 \pm 0.10$	(4,3,3)
0841+129	2.476	$-1.22 \pm 0.23$	$\geq -1.85$	$-1.84 \pm 0.10$	$-1.60 \pm 0.11$	$\leq -1.63$	(3,3,3)
1215+333	1.999	$< -1.37$	$-1.47 \pm 0.08$	$\geq -1.81^{\text{d}}$	$-1.50 \pm 0.08$	$-1.31 \pm 0.09$	(3,3,3)
2231–0015	2.066	$\geq -0.93$	$-0.86 \pm 0.10$	$-1.32 \pm 0.10$	$-1.07 \pm 0.11$	$-0.75 \pm 0.10$	(3,3,3)

NOTES—All abundances have been normalised to the meteorite values reported by Anders & Grevesse (1989):  $\log (\text{S}/\text{H})_{\odot} = -4.73 \pm 0.05$ ,  $\log (\text{Si}/\text{H})_{\odot} = -4.45 \pm 0.02$ ,  $\log (\text{Fe}/\text{H})_{\odot} = -4.49 \pm 0.01$ ,  $\log (\text{Cr}/\text{H})_{\odot} = -6.32 \pm 0.03$ ,  $\log (\text{Zn}/\text{H})_{\odot} = -7.35 \pm 0.02$ . Errors in  $[\text{X}/\text{H}] = \log (\text{X}/\text{H})_{\text{obs}} - \log (\text{X}/\text{H})_{\odot}$  include errors in X and H column densities and errors in solar abundances.

<sup>a</sup>From SII column densities obtained in this paper

<sup>b</sup>From SiII column densities given in Prochaska & Wolfe 1999

<sup>c</sup>References for the column densities of FeII, CrII, & ZnII respectively

<sup>d</sup>Prochaska & Wolfe 1999 gave  $\log N(\text{FeII}) = 14.65 \pm 0.04$  derived from the saturated transition FeII 1608, and they warn that  $N(\text{FeII})$  must be underestimated, hence we use this value as a lower limit

REFERENCES—(1) Ge & Betchold (1997); (2) Pettini et al. (1994); (3) Prochaska & Wolfe 1999; (4) This paper

Table 4.  $[\alpha/\text{iron-peak}]$  abundance ratios in DLAs

QSO	$z_{\text{abs}}$	[S/Zn]	[Si/Fe]	[Si/Fe] <sub>corr</sub>
0013–004	1.973	$-0.39 \pm 0.14$	...	...
0100+1300 <sup>a</sup>	2.309	$-0.04 \pm 0.08$	$+0.37 \pm 0.07$	+0.15
0347-3819 <sup>b</sup>	3.025	$\geq -0.37$	$+0.31 \pm 0.03$	...
0149+3335	2.141	$\leq +0.68$	$+0.13 \pm 0.04$	+0.03
0528–2505 <sup>c</sup>	2.811	$-0.12 \pm 0.09$	$+0.51 \pm 0.12$	+0.10
0841+129	2.374	$+0.18^{+0.18}_{-0.21}$	$+0.37 \pm 0.24$	+0.23
0841+129	2.476	$> +0.20$ <sup>d</sup>	$> -0.01$	...
1215+333	1.999	$< +0.46$	$\leq +0.34 \pm 0.2$	...
1331+170 <sup>e</sup>	1.776	$-0.11 \pm 0.11$	$+0.65 \pm 0.10$	+0.00
2231–0015	2.066	$\geq -0.18$	$+0.46 \pm 0.03$	+0.04
2348–147 <sup>f</sup>	2.279	$\geq -0.89$	$+0.37 \pm 0.02$	...

NOTES— Relative abundances  $[X/Y]$  have been directly obtained from the column densities of  $X^+$  and  $Y^+$  species (references in Table 3, otherwise indicated) and using the meteoritic values of Anders and Grevesse 1989. Errors in  $[X/Y]$  take into account error in  $X^+$  and  $Y^+$  column densities and errors in solar abundances.  $[\text{Si}/\text{Fe}]_{\text{corr}}$  are ratios corrected by dust effects following Vladilo (1998).

<sup>a</sup>N(SII) from MCV98; N(ZnII), N(FeII) from Prochaska & Wolfe 1999; N(SiII) from Lu et al 1998

<sup>b</sup>N(SII) from Centuri3n et al. 1998; N(ZnII) from Pettini et al. 1994; N(SiII) and N(FeII) from Prochaska & Wolfe 1999

<sup>c</sup>N(SII), N(SiII), N(ZnII), N(FeII) from Lu et al. 1996

<sup>d</sup>The most conservative value by using  $\log N(\text{SII})=14.81-0.21$  see Table 2

<sup>e</sup>N(SII) from Kulkarni et al 1996, N(ZnII), N(SiII), N(FeII) from Prochaska & Wolfe 1999

<sup>f</sup>N(SII), N(SiII), N(FeII) from Prochaska & Wolfe 1999; N(ZnII) from Pettini et al. 1994;